Maturation Stages of Mouse Dendritic Cells in Growth Factor–dependent Long-Term Cultures

By Claudia Winzler,* Patrizia Rovere,§ Maria Rescigno,* Francesca Granucci,* Giuseppe Penna,‡ Luciano Adorini,‡ Valerie S. Zimmermann,§ Jean Davoust,§ and Paola Ricciardi-Castagnoli*

*From the *CNR Centre of Cellular and Molecular Pharmacology, Milan 20129, Italy; ‡Roche Milano Ricerche, Milan 20132, Italy; §Centre d'Immunologie INSERM-CNRS de Marseille Luminy, Parc Scientifique de Luminy, Case 906, Marseille 13288, France*

Summary

The signals controlling the checkpoints of dendritic cells (DC) maturation and the correlation between phenotypical and functional maturational stages were investigated in a defined model system of growth factor–dependent immature mouse DC. Three sequential stages of DC maturation (immature, mature, and apoptotic) were defined and characterized. Immature DC (stage 1) had low expression of costimulatory molecules, highly organized cytoskeleton, focal adhesion plaques, and slow motility; accordingly, they were very efficient in antigen uptake and processing of soluble proteins. Further, at this stage most of major histocompatibility complex class II molecules were within cytoplasmic compartments consistent with a poor allostimulatory capacity. Bacteria or cytokines were very efficient in inducing progression from stage 1 towards stage 2 (mature). Morphological changes were observed by confocal analysis including depolymerization of F-actin and loss of vinculin containing adhesive structures which correlates with acquisition of high motility. Antigen uptake and presentation of native protein antigen was reduced. In contrast, presentation of immunogenic peptides and allostimulatory activity became very efficient and secretion of IL-12 p75 was detectable after antigen presentation. This functional DC maturation ended by apoptotic cell death, and no reversion to the immature phenotype was observed.

Dendritic cells (DC)[1] comprise a family of professional APC responsible for the activation of naive T cells and the generation of primary T cell responses (1). To fully perform these functions, DC residing in non-lymphoid tissues need to be activated and to initiate a differentiation process. This maturation of DC is characterized by profound changes in MHC class II distribution, antigen-processing capacity (2), expression of costimulatory molecules (3) and a marked rearrangement of adhesion molecules that is likely to allow DC migration to lymphoid organs (4). DC maturation should be critically controlled by microenvironmental signals. However, limited knowledge exists about the factors and the mechanisms regulating DC cell cycle, life span, and functional activity. Cytokines secreted in a paracrine (e.g., GM-CSF, TNFα) or autocrine (TNFα, IL-1β) fashion control DC movements (4), survival (5), and APC activity (6, 7), but the fine biochemical mechanisms underlying these effects are not known. Once DC have interacted with T cells, they complete the differentiation process, which is believed to terminate by apoptosis.

Several groups have succeeded in generating large numbers of functional DC/Langerhans cells (LC) in both the murine or the human system by treating DC precursors with GM-CSF alone or in combination with other growth factors (8–13). However, such DC could be propagated only for limited time periods, i.e., up to 3 mo. More recently, growth factor-dependent long-term DC lines from mouse fetal or newborn skin have been established (14, 15). Nevertheless, although these lines possess the properties of DC precursors and maintain an immature phenotype they cannot be induced to mature in vitro (14, 15).

Here we present evidence that MHC class II–positive growth factor–dependent immature DC, derived from adult mice spleen, can be driven in vitro to proliferate over more than one year of continuous culture. Proliferation and survival of such immature cells are strictly dependent upon the presence of exogenous GM-CSF and fibroblast-derived growth factors. Long-term DC preserve an immature phenotype but various activating signals, such as living bacteria

[1] *Abbreviations used in this paper:* DC, dendritic cells; LC, Langerhans cells; SN, supernatant.

or cytokines, promote full maturation. During this process, class II molecules are exported at the cell surface, adhesion/costimulatory molecules are upregulated, the actin-based cytoskeleton is rearranged, and cell motility is increased. Furthermore, only matured cells are able to activate antigen-specific T cells and to produce IL-12 p75, a key cytokine skewing the response towards a Th1 polarization.

Using this novel in vitro differentiation system, kinetic stages of DC maturation and apoptotic cell death could be established. On the basis of the results of this study and previous data from the literature, a model of DC maturation checkpoints and sequential events is proposed.

Materials and Methods

Animals. Mice were purchased from Charles River Laboratories (Calco, Como, Italy). To obtain DC cultures female C57BL/6 mice were used at 6–10 wk of age. For the MLR assay, female BALB/C mice at 2–4 mo of age were used as source of lymph-node cells.

Culture Media. Culture medium was IMDM (Sigma Chem. Co., St. Louis, MO) containing 10% heat-inactivated FBS (Hyclone, Logan, Utah), 100 IU/ml penicillin, 100 μg/ml streptomycin, 2 mM L-glutamine (all from Sigma), and 50 μM 2-βME (complete IMDM). Fibroblast supernatant (SN) from NIH/3T3 cells was collected from confluent cultures and filtered (0.2 μ; Corning Glass Works, Corning, NY).

Cytokines and Bacteria. Recombinant murine GM-CSF was purchased from PharMingen (San Diego, CA). Recombinant human IL-2 was from R&D Systems (Wiesbaden, Germany). Murine rTNFα (Genentech Inc., San Francisco, CA) was used at 100 U/ml. Murine rIL-1β and rIL-6 were purchased from Genzyme (Cambridge, MA) and used at 10 ng/ml. *Escherichia coli* ($Gram^-$) and *S. aureus* ($Gram^+$) bacteria were kindly provided by G. Pozzi and D. Medaglini (University of Siena, Italy). In experiments of DC stimulation, bacteria: DC ratio was 1:1. DC cells were cultured with living bacteria for 18 h before analysis. LPS (*E. coli* 026:B6 from Sigma) was used at 1 μg/ml.

Generation of DC Cultures. Spleens from 6–10-wk-old female C57BL/6 mice were used. Single cell suspensions were obtained by gentle teasing with forceps and filtered with a cell strainer. Erythrocytes were lysed by treatment with ammonium chloride. Remaining unfractionated cell populations were plated at a density of 5×10^5 cells/ml in suspension culture Petri dishes (Corning Glass Works, Corning, NY). Culture medium for generation and expansion of DC was complete IMDM supplemented with 30% NIH/3T3 SN containing 10–20 ng/ml mouse rGM-CSF (we refer to this conditioned medium as R1 medium). Cultures were fed with fresh R1 medium every 3–4 d. First passages of DC-enriched cultures were performed after ~2 wk. Both suspended and weakly adherent cells were propagated. Clusters of adherent cells with dendritic morphology were detached using PBS with 3 mM EDTA. The remaining strongly adherent cells were discarded. After 3 mo of culture, cells could be passaged every week. Experiments were performed with cells continuously cultured for more than 12 mo. This homogeneous, growth factor–dependent DC population, is referred to as D1 cells.

In experiments using rTNFα, culture medium was changed before the experiment and fresh rTNFα (100 U/ml) was added every 24 h. Similarly, rM-CSF and rGM-CSF were used at a concentration of 20 ng/ml.

Antibodies. Biotin-labeled N418 specific for CD11c was prepared as described (16). Hybridoma 2.4G2 (rat anti–mouse FcγII/III receptor, CD32) was a kind gift from B. Kyewski (DKFZ, Heidelberg, Germany). Biotinylated anti-F4/80 was purchased from Serotec (Oxford, UK). The following biotinylated mAbs were from PharMingen: H-$2K^b$ (AF6-88.5), H-$2D^b$ (28-14-8), CD80/ B7.1 (1G10), CD11a/LFA-1 (2D7), CD11b/Mac-1 (M1/70), CD54/ICAM-1 (3E2), CD45 (M1/9.3), CD117/c-kit (3C1) B220 (RA3-6B2), and CD4 (RM4-5) FITC-conjugate HM40-3 specific for CD40 and rat IgM J11d (heat-stable antigen [HSA]) (both from PharMingen). Anti–class II (I-$A^{b,d}$) hybridoma (34-5-3S) was purchased from the American Tissue Culture Collection (ATCC, Rockville, MD) and biotinylated. PE-conjugated 2G9 (PharMingen) was used for staining I-A/Ed. FITC-coupled GL1 (PharMingen) was used for staining of CD86/B7.2. Rabbit polyclonal antibodies anti-c-fms/CSF1R (C20) and anti-FAS-L (Q20) were from Santa Cruz Biotechnology; hamster polyclonal anti-FAS antibody was from Pharmingen. PE-conjugated and FITC-conjugated donkey anti–mouse and Texas red-conjugated donkey anti–rabbit Ig were from Jackson ImmunoResearch (West Grove, PA). PE-streptavidin, FITC-conjugated extravidin, and FITC-goat anti–rabbit IgG were purchased from Sigma. Mouse adsorbed goat anti–rat Ig FITC and goat anti–hamster IgG-PE were from Southern Biotechnology (Birmingham, AL). Mouse anti–rat IgM FITC and isotype-matched control antibodies were from PharMingen. Anti-vinculin and anti-tubulin mAbs and rodhamin-conjugated phalloidin were a generous gift of P. Chavrier (Centre d'Immunologie de Marseille Luminy [CIML], Marseille, France) and were used at the final concentration of 1 μg/ml. Anti-murine H2-Mβ polyclonal rabbit antibody was kindly provided by N. Barois (CIML). Before labeling experiments, FcR blocking was performed by incubating cells with 5% normal mouse serum or 2.4G2 (anti-CD32) supernatant.

Cell Surface Phenotype. Both suspended and adherent cell populations were harvested and analyzed. Adherent cells were detached with PBS buffer containing 3 mM EDTA (3 min 37°C). Staining was performed according to standard immunofluorescence techniques. Aliquots of cells (1.5×10^5/sample) were preincubated for 30 min on ice with undiluted 2.4G2 SN to prevent binding to FcγRII/III. Cells were then exposed to FITC-coupled GL1, FITC-coupled HM40-3, PE-conjugated 2G9, biotinylated mAbs (all used at 10–20 μg/ml), or J11D culture SN for 30 min on ice. Appropriately diluted FITC-streptavidin, PE-streptavidin, or FITC-conjugated mouse anti–rat IgM, respectively, were used to detect binding of biotinylated mAbs. When 2.4G2 hybridoma culture SN were used as first step reagent, binding of antibody was detected by FITC-coupled goat anti–rat Ig. After every incubation step, samples were washed with PBS containing 0.1% sodium azide and 2% FCS. Flow cytometry analysis was performed with a FACScan® (Lysis I software; Becton Dickinson). For sorting experiments, sodium azide containing antibodies were dialyzed against IMDM and sterile filtered before use. Cell sorting was performed with a FACS® Vantage (Becton Dickinson) using the Lysis I program. Cells were gated for size and side scatter to exclude dead cells and debris.

Detection of Apoptosis. Cells in log phase of growth were thoroughly washed out from GM-CSF and fibroblast-conditioned culture medium. 6×10^5 cells were replated in 5 ml of medium without cytokines and SN or, for control stainings, in fully supplemented culture medium. At different time points (24–72 h) after growth factor deprivation, cytospins were prepared and slides fixed in acetone. To detect cells containing DNA fragments, the TUNEL (TdT-mediated dUTP nick-end labeling) method was

employed with the modifications suggested by the supplier (DIG Oligonucleotide 3′-End Labeling Kit; Boehringer Mannheim, Germany). Slides were rinsed three times in PBS and kept for 30 min at room temperature protected from light in humid atmosphere with 20 μg/ml rhodamine-labeled sheep anti-digoxigenin antibody Fab fragments (Boehringer Mannheim). Three washing steps in PBS followed to eliminate unbound antibody. Stained samples were mounted in Fluoromount G (Southern Biotechnology).

Intracellular Immunofluorescence. To visualize the intracellular distribution of class II molecules and of cytoskeleton elements, 48 h TNFα-treated D1 cells were seeded on polylysin-coated coverslips for 20 min at room temperature. After adhesion, cells were washed and incubated for 20 min at 37°C in culture medium. Control cells were incubated over night on glass coverslips. Fixation was performed for 15 min at room temperature in 4% (wt/vol) paraformaldehyde in PBS. In selected experiments, to preserve the microtubules organization, cells were fixed with 3% paraformaldehyde, 0.3% glutaraldehyde, and incubated for 5 min at room temperature in a $NaBO_4$ buffer (100 mM, pH 7.4) before permeabilization. Fixed cells were washed three times in PBS containing 10 mM glycine, 0.1 mM $MgCl_2$, and 0.1 mM $CaCl_2$, permeabilized for 30 min at room temperature with 0.5% (wt/vol) saponin, in PBS/0.2% BSA. For class II compartment characterization, coverlips were incubated for 30 min at room temperature with 5 μg/ml mouse anti–I-$A^{b,d}$ class II (34.5.3S) and 5 μg/ml rabbit anti-H2-Mβ Abs, washed and then incubated for 30 min at room temperature with 10 μg/ml FITC-conjugated donkey anti–mouse and 10 μg/ml Texas red-conjugated donkey anti–rabbit Abs.

To visualize the cytoskeleton organization coverslips were incubated for 30 min at room temperature with anti-vinculin (1 μg/ml) or anti-tubulin (1 μg/ml) mAbs, washed, and then incubated for additional 30 min at room temperature with 10 μg/ml FITC-conjugated donkey anti–mouse antibodies in the presence or absence of rhodamine-labeled phalloidin to visualize F-actin. Before mounting in Moviol (Sigma), samples were washed three times in staining buffer and once in distilled water. Cell morphology was analyzed by confocal microscopy using reflection interference contrast. Confocal laser scanning microscopy was performed using a Leica TCS 4D (Leica Lasertechnik, Heidelberg, Germany) as described (17, 18). A focal series of four horizontal or vertical planes of section spaced by 0.75 mm were monitored simultaneously for fluorescein and Texas red/rhodamine, using the 488 and 568 nm laser lines of an argon-krypton, a double dichroic mirror for the excitation beam, a FITC band pass 520–560-nm barrier filter and a long pass barrier filter above 580 nm for Texas red/rhodamine detection, using green-sensitive and red-sensitive photomultipliers, respectively. The FITC/Texas red 8 bits-encoded 1024 × 1024 pixel images from the same plane of section were superimposed and visualized with a green/red pseudocolorscale on a true color display monitor before printing using a Codonics NP-1600 dye-sublimation color printer (Codonics, Middleburg Heights, OH).

Time-Lapse Videomicroscopy. D1 cells were continuously recorded for 16 h with a Zeiss Axiovert microscope equipped with a small incubator (37°C) and video camera, through the courtesy of Fabrizio Manca and Daniele Severino (University of Genova, Italy). TNFα (100 U/ml) was added to the D1 culture after the first 2 h of recording.

Endocytosis. Ovalbumin (OVA) and Dextran (40,000 dalton) were purchased from Sigma and conjugated with FITC, as described (19). Cells were grown in culture medium in the presence or absence of 100 U/ml mrTNF-α. After 48 h, cells were incubated at 37°C or at 0°C for 1 h with 0.1–1 mg/ml FITC-OVA, or FITC-Dextran (FITC-DX). Uptake was stopped by adding ice-cold FACS® buffer followed by three washes in ice-cold PBS with 5% BSA and 0.02% sodium azide. After staining with the anti–class II mAb (30 min on ice) cells were analyzed by flow cytometry using a FACScan® (Becton-Dickinson, San Jose, CA).

Mixed Leukocyte Reaction Assay. Primary allogeneic MLR was set up with I-A^{bright} and I-A^{int} sorted DC as stimulators one day after FACS® sorting. Stimulator cells were treated with mitomycin C (50 μg/ml, 20 min at 37°C; Sigma) and cocultured with 2×10^5 BALB/c lymphnode cells/well in 200 μl of complete IMDM. Cultures were pulsed on day 3 with 1 μCi/well of [^{3}H]thymidine (specific activity 2.0 Ci/mmol; Amersham, Amersham Place, UK). Incorporation of [^{3}H]thymidine was measured 18 h later with a liquid scintillation counter (MicroBeta Plus; Wallac, Turku, Finland). Each point in the graphs represents the mean cpm from triplicate cultures.

Antigen Presentation Assay. TNFα-treated (100 U/ml) or untreated D1 (1×10^4 cells/well) were seeded in flat-bottomed microtiter plates (Corning) pulsed with OVA protein (grade III; Sigma) or peptide 327-339 (kindly synthesized by R. Longhi, CNR, Milan, Italy) and cultured together with the T cell hybridoma BO97.10 (5×10^4 cells) specific for OVA/A^b (20) in complete IMDM in a final volume of 200 μl/well. Plates were incubated for 24 h at 37°C with 5% CO_2. Aliquots of supernatants were harvested and frozen before measuring IL-2 content. CTLL-2 were grown in 100 U/ml rIL-2 and extensively washed before being added to thawed supernatants. CTLL-2 cells (10^4 cells/well) were incubated for 24 h with 50 μl of the supernatants in a 150 μl final vol/well and pulsed with 1 μCi/well of [^{3}H]thymidine (specific activity 5.0 Ci/mmol; Amersham) for additional 6 h. Incorporation of [^{3}H]thymidine by CTLL-2 cells was measured by liquid scintillation counting. Each point in the graphs represents the mean cpm from triplicate cultures.

IL-12 Production. IL-12 p75 production by D1 cells was measured following antigen presentation. In brief, TNFα-treated (100 U/ml) or untreated D1 cells (1×10^4 cells/well) were seeded in flat-bottomed microtiter plates, pulsed with OVA protein (grade III; Sigma) or peptide 327-339 and cultured together with 5×10^4 BO97.10 T cell hybridoma specific for OVA/A^b in complete IMDM in a final volume of 200 μl/well. After 24 h culture at 37°C in 5% CO_2 supernatants were tested for IL-12 p75 content. Polyvinyl microtiter plates (Falcon 3012) were coated with 100 μl of the rat anti–mouse IL-12 heterodimer 9A5 mAb, in carbonate buffer. After blocking, 50 μl/well of samples were diluted in test solution (PBS containing 5% FCS and 1 g/l phenol) and incubated together with 50 μl peroxidase-conjugated 5C3 mAb (rat anti–mouse IL-12 p40 subunit). Anti-IL-12 antibodies (21) were kindly provided by Dr. M.K. Gately (Hoffmann-La Roche Inc., Nutley, NJ). After overnight incubation at 4°C, bound peroxydase was detected by 3,3′-5,5′-tetramethylbenzidine (Fluka Chemical Co.), and adsorbance read at 450 nm with an automated microplate ELISA reader (MR5000; Dynatech). IL-12 p75 was quantified from two to three titration points using standard curves generated by purified recombinant mouse IL-12 and results expressed as cytokine concentration in pg/ml. Detection limit was 10 pg/ml.

Results

Generation of Long-term Immature DC from Cultured Mouse Spleen Cells. DC were derived from spleen cell suspen-

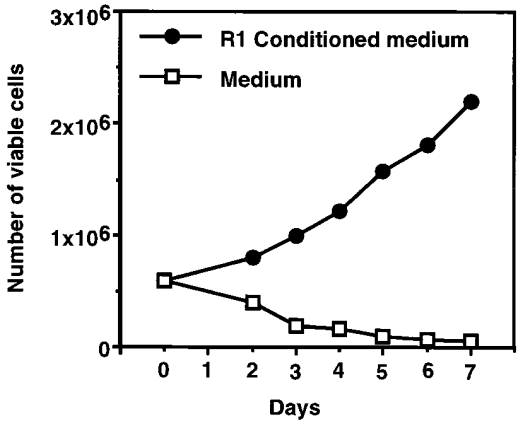

Figure 1. Growth curve of D1 cells in the presence of conditioned medium (R1) or growth factors deprived (medium alone).

sions cultured in medium supplemented with fibroblast supernatant, known to support the growth of skin DC (22), together with GM-CSF, a cytokine essential for DC growth.

Typical adherent aggregates of DC with fine membrane projections were visible at the periphery of the clusters on day 10–12 and in the following days both cell clusters and DC increased in number and size. The first passage was performed around days 12–14 using EDTA treatment to leave behind only the strongly adherent cells. After 10–12 wk, cultures consisted of single adherent cells with fine cytoplasmic protrusions, adherent cell clusters and cells growing in suspension, some of which had veiled morphology. Cell growth could be continuously maintained (at least over one year) but was strictly dependent on the presence in the culture medium of GM-CSF and fibroblast supernatant (R1 medium). Growth factor deprivation led to cell growth arrest and cell death (Fig. 1). DNA fragments in apoptotic cells were visualized by TUNEL staining, starting from 24–48 h after deprivation, with a number of viable cells decreasing to less than 10% after 1 wk (data not shown). After 6 mo of continuous growth this long-term bulk culture of spleen DC was named D1. The method is highly reproducible given that additional long-term growth factor–dependent DC lines have been independently generated using the same approach.

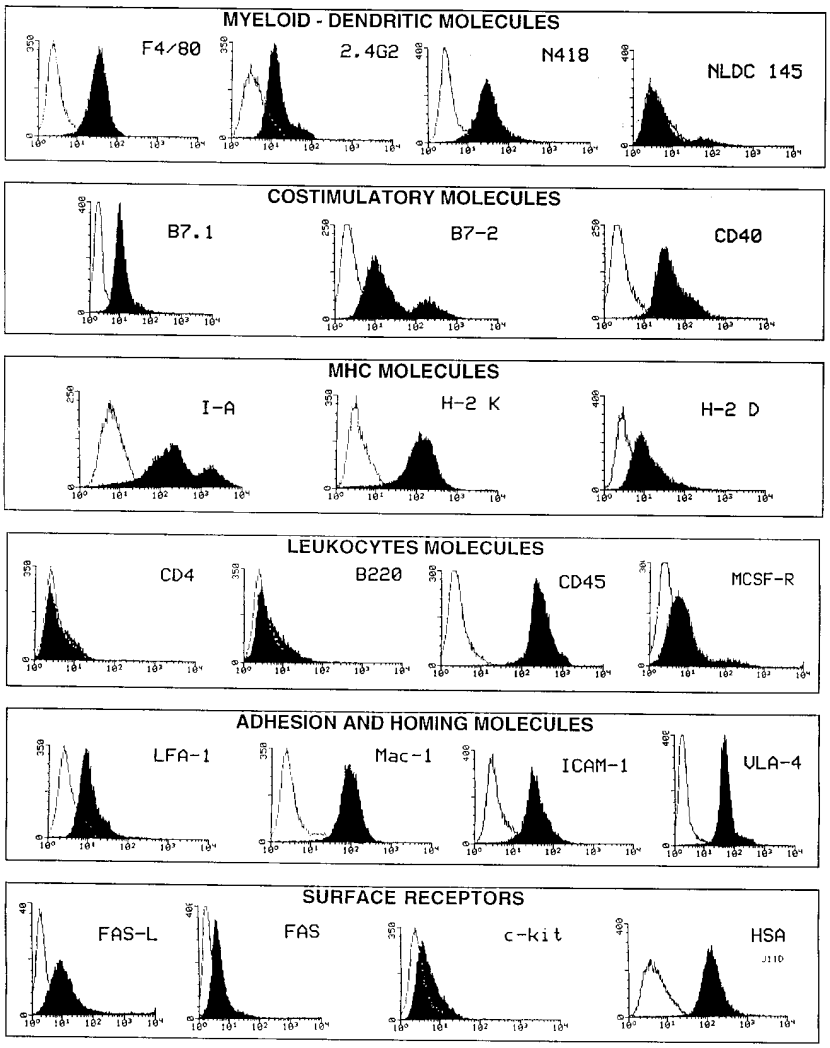

Figure 2. Surface markers of D1 bulk culture by FACS® analysis. Filled histograms are showing binding of specific antibodies, whereas isotype matched control antibodies or secondary reagents are represented by open histograms. Cell surface phenotype was assessed with antibodies as indicated in Materials and Methods. Before all labeling experiments, FcR blocking was performed by incubating cells with 5% normal mouse serum or anti FcR (2.4G2) mAb.

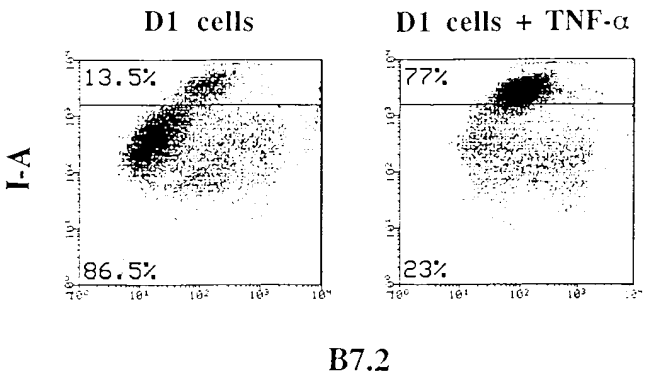

Figure 3. Dot plot double-color FACS® analysis of MHC class II and B7.2 molecules of D1 bulk culture.

D1 Cells Preserve the Phenotype of Immature DC, and Cannot Be Converted to Macrophages in Response to M-CSF. Surface markers expressed in D1 cultures included CD11c (N418), FcγII/III receptor (2.4G2), and F4/80; NLDC145 was expressed only in ~10% of the cells (Fig. 2). The majority of the cells expressed moderate levels of membrane class II molecules (I-A^{int}), but 20% of the cells expressed high levels (I-A^{bright}) of class II molecules. The same staining pattern, albeit at lower fluorescence intensity, was observed for B7.2. Double-color flow cytometric analysis of unstimulated cells showed that I-A^{bright} cells were those expressing higher levels of B7.2 (Fig. 3). D1 were positive for all class I antigens (H-2 K, D), and for the costimulatory CD40 and B7.1 molecules (Fig. 2). Adhesion and homing receptors such as CD11a (LFA-1), CD11b (Mac-1), CD54 (ICAM-1), and VLA-4 were highly expressed, as well as the heat stable antigen (HSA/J11d). In contrast, granulocytes, T and B cell markers were negative (Fig. 2), whereas c-kit and Fas ligand were expressed, although at low levels. Interestingly, the M-CSF receptor c-fms (CD115) was also expressed but experiments aimed at converting the D1 cells to a macrophage phenotype by adding rM-CSF in culture, showed that substitution of rGM-CSF (or R1 supernatants) with M-CSF (or M-CSF supplemented with fibroblast supernatant) in the culture medium, reduced the D1 cell via-

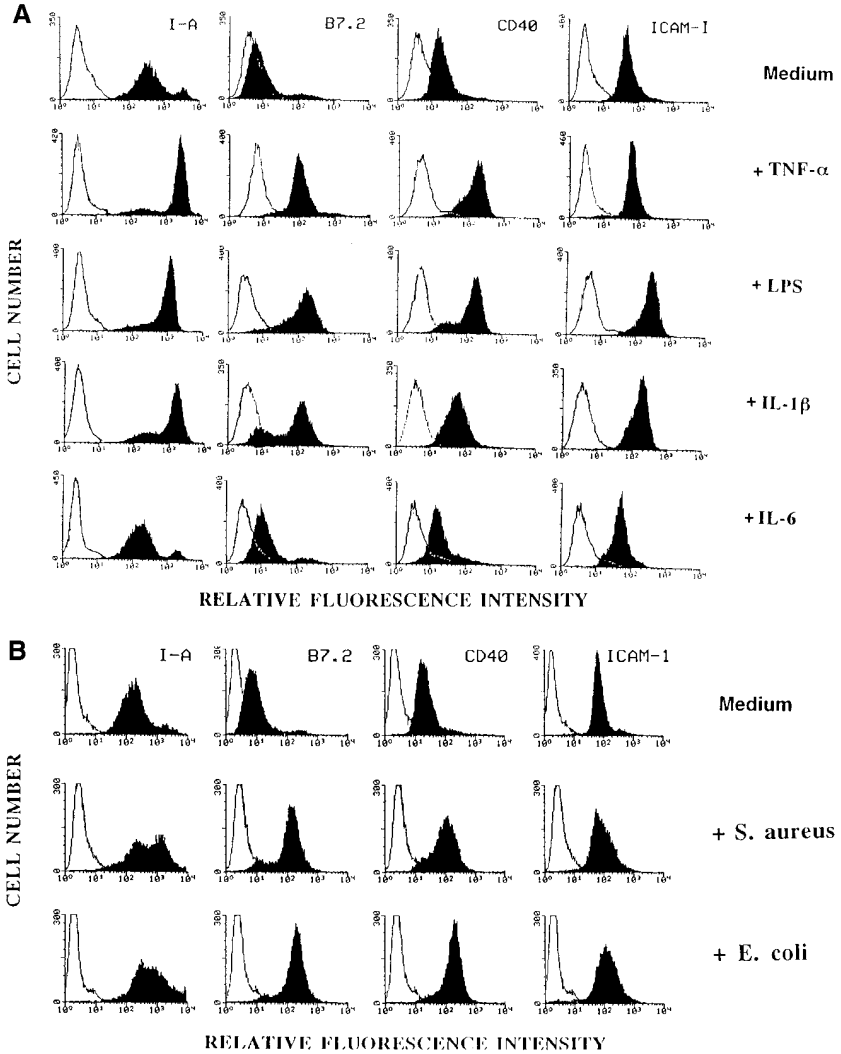

Figure 4. Phenotypical maturation of D1 cells. Surface markers by FACS® analysis after cytokine or living bacteria treatment. MHC class II (I-A), B7.2, CD40, and ICAM-1 molecules of D1 bulk culture growing in R1 medium or in medium supplemented with TNFα, LPS, IL-1β, or IL-6 (*A*) or after treatment with living *E. coli* or *S. aureus* (*B*).

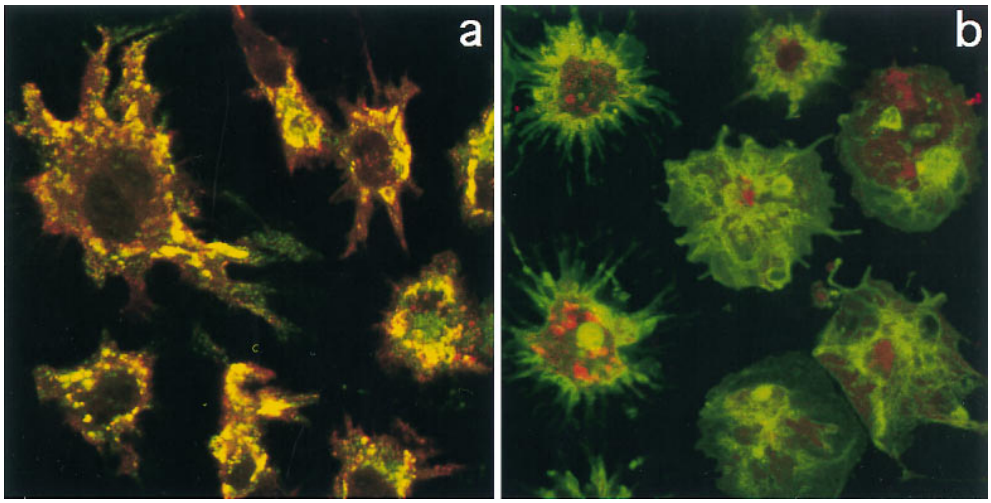

Figure 5. Redistribution of MHC class II molecules during maturation. Double-color confocal laser scanning microscopy analysis of class II–containing compartments in immature (*a*) and mature (*b*) D1 cells. Class II–positive (*green*) and H2-Mβ-positive (*red*) vesicles are mostly colocalized (*yellow*) in untreated D1 cells (*a*). Treatment of the cells with TNFα induces the redistribution of class II molecules from the cytoplasm to the cell surface (*b*) and no colocalization between class II (*green*) and H2-Mβ (*red*) containing vesicles can be observed.

bility to 15%, in 3 d. Growth arrest was observed in the remaining viable cells, which survived only for a few weeks. Altogether these results indicate that mouse spleen DC, grown in the culture conditions listed above, preserve the phenotype characteristic of immature DC.

Phenotypic Maturation of DC Can Be Induced by Microbes, LPS or Cytokines such as TNFα and IL-1β, but not IL-6. Floating cells with veils and dendrites were seen in unstimulated cultures only at low frequency and most of the cells appeared to be loosely adherent to the surface of the culture dish. When cells were treated daily with 100 U/ml TNFα for 1–4 d, they detached from plastic surface, developed larger veils and longer dendrites, and formed large floating cell aggregates (data not shown). These morphological changes were also easily observed by time-lapse videomicroscopy (see below).

TNFα, LPS, IL-1β, and IL-6 were tested for their ability to modulate the expression of markers involved in APC/T cell interactions and differentially expressed in immature versus mature DC. Cells were stimulated for 24 h with either 100 U/ml TNFα, 1 μg/ml LPS or 10 ng/ml IL-1β, stained, and then analyzed by flow cytometry. I-A, B7.2, CD40, and ICAM-1 molecules were strongly upregulated by all stimuli, whereas expression of the same surface molecules did not change after treatment with 10 ng/ml IL-6 (Fig. 4 *A*).

Gram$^+$ (*S. aureus*) and Gram$^-$ (*E. coli*) living bacteria were also used to activate immature D1 cells. Both types of bacteria induced upregulation of MHC class II, B7.2 and CD40 molecules, whereas ICAM-1 was unchanged (Fig. 4 *B*).

Mature I-A^{bright} DC Are Derived from Immature I-A^{int} Cells. To ascertain whether the I-A^{bright} cells were deriving from the I-A^{int} cells, the two populations were FACS®-sorted and then cultured again after sorting. Analysis of surface I-A expression after 6 d of culture showed that previously sorted I-A^{int} cells included again a small population of I-A^{bright} cells (data not shown). Because previous experiments showed that LPS increased surface expression of I-A molecules, culture medium was examined for traces of endotoxin content as a possible explanation for this apparently spontaneous in vitro maturation. Indeed, a very low amount (~0.3 ng/ml) of endotoxin was detected in the standard R1 culture medium, thus suggesting that the observed spontaneous DC maturation may be due to LPS.

Sorted I-A^{bright} cells replated in culture displayed a morphology similar to those treated with TNFα, including formation of floating aggregates. However, I-A^{bright} cells could not be propagated in culture, and >90% of these sorted cells could not be rescued after 6 d of culture. Neither addition of TNFα nor addition of the R1 supernatant improved the viability of I-A^{bright} sorted cells (data not shown). This finding indicates that DC maturation is an irreversible process and that when particular checkpoints are passed, maturation can not be reverted. This is also suggested by the impossibility to propagate long-term DC purified on the basis of high MHC class II expression.

Redistribution of MHC Class II Molecules and Their Export to the Cell Surface Membrane Correlates with DC Maturation. Confocal microscopy after staining with anti-class II mAbs revealed that unstimulated cells express high amounts of class II molecules. However, consistent with the results of FACS® analysis, most of them were not at the cell surface but were contained in discrete intracellular vesicular compartments (Fig. 5 *a*). A minor cell population, (~15%), exhibited a more pronounced DC morphology and were stained more strongly at the cell surface and less intracellularly (not shown). To better define the characteristics of these intracellular class II positive compartments, double staining with anti-H2-Mβ antibody was performed. Class II positive vesicles appear to colocalize with H2-Mβ-positive vesicles in immature D1 cells (Fig. 5 *a*, yellow color due to the superimposition of green class II–containing vesicles and red H2-Mβ-containing vesicles). These results indicate that mature class II molecules, exported from the *trans*-Golgi network, are mostly located in a compartment similar to the MIIC, and to the prelysosomal compartments defined in B cells. In contrast, maturation of D1 cells with TNFα, induced a redistribution of class II molecules at the cell sur-

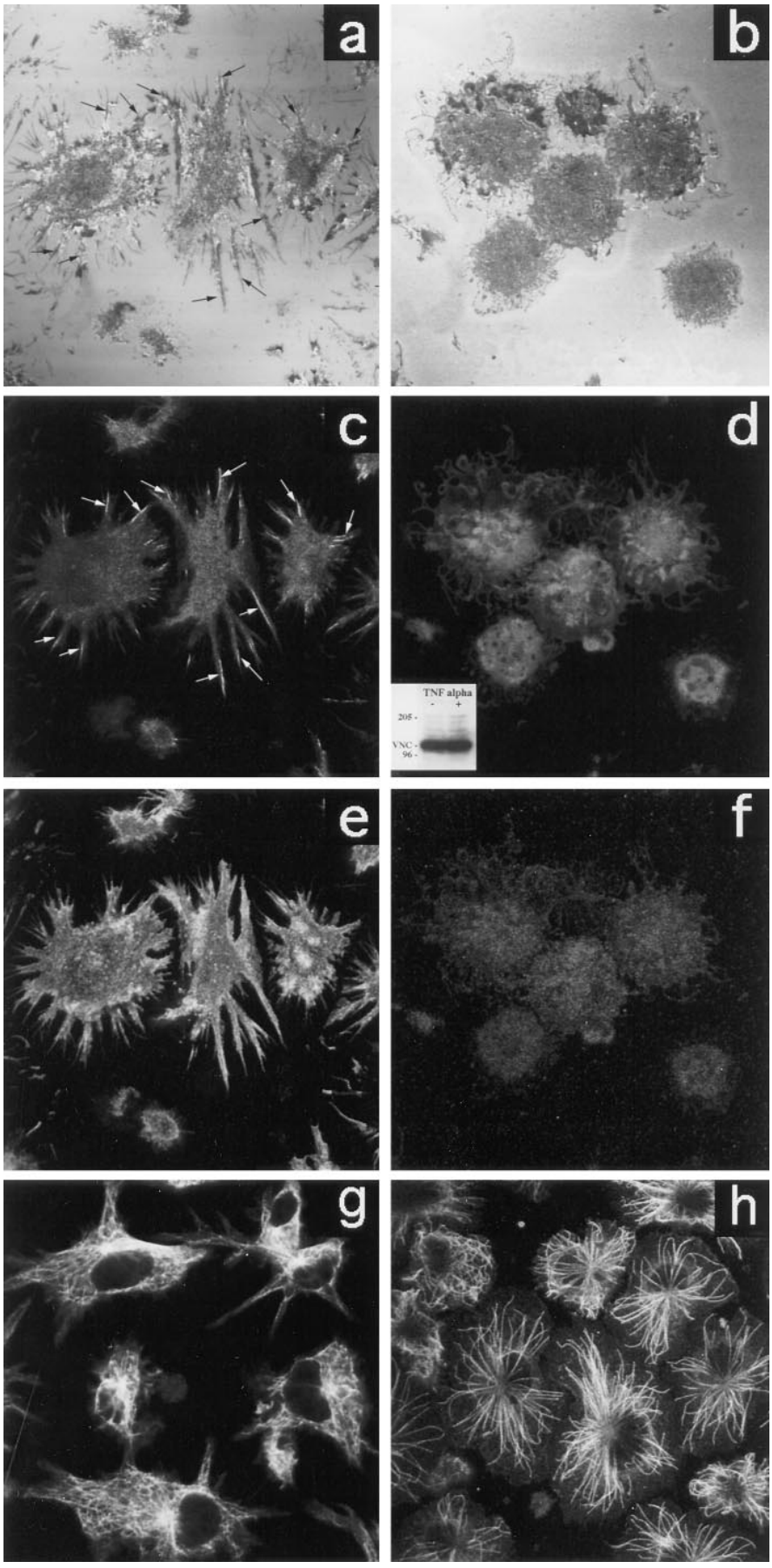

Figure 6. Cytoskeleton modifications in D1 cells after TNFα treatment. Immature (*a*) and mature (*b*) D1 cells morphology was analyzed by confocal microscopy using reflection interference contrast which gives the best visualization of the cell interface zone when attached to a glass support (37). Confocal laser scanning microscopy of D1 cells stained with anti-vinculin (*c* and *d*), phalloidin (*e* and *f*), and anti-tubulin (*g* and *h*) was also performed. Immature D1 cells (*a*, *c*, *e*, and *g*) appear to be adherent (*a*) and characterized by: vinculin containing adhesive structures (*a* and *c*, *arrows*), subcortical actin aggregates (*e*), and highly organized tubulin (*g*). D1 treatment with TNFα (*b*, *d*, *f*, and *h*) clearly induces morphological modification (*b*). Mature D1 cells lose adherence (*b*), vinculin (*d*), and subcortical actin organization (*f*). No differences in the amount of vinculin protein are detectable by Western blot analysis (*d*, *inset*). Microtubules are only partially affected by TNFα treatment (*h*).

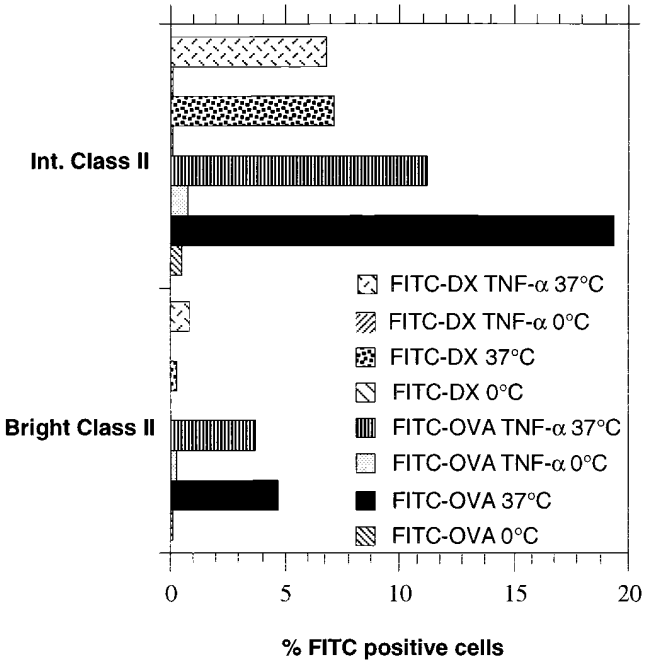

Figure 7. Antigen uptake (FITC-OVA and FITC-DX) by D1 bulk population in the presence or absence of TNFα was analyzed by double-color FACS® analysis. The D1 cells that better internalize soluble antigens at 37°C expressed comparatively low levels of MHC class II molecules, whereas class II^{bright} were less efficient in both FITC-OVA and FITC-DX uptake. Incubation of the cells with TNFα reduced the protein uptake of the immature D1 subpopulation and had no effects on the mature D1 subpopulation.

face. Although intracellular class II staining was still observed no colocalization with H2-Mβ molecules was visualized (Fig. 5 *b*, green class II–containing vesicles and red H2-Mβ-containing vesicles do not colocalize). This result suggests that DC maturation involves a redistribution of MHC class II molecules: fully mature D1 cells have class II molecules expressed mostly at the cell surface and only partially in intracellular compartments.

Rearrangement of Microfilaments and of Microtubules Correlates with DC Functional Maturation. Cell migration requires a coordinate series of events that include a sequential rearrangement of both surface adhesion molecules and of the actin-based cytoskeleton. Immature D1 cells are characterized by numerous membrane expansions that terminate in adhesive structures displayed in the panel by black arrows (Fig. 6 *a*). Highly organized vinculin can be visualized in the adhesive structures (Fig. 6 *c*, *arrows*). These structures are also characterized by the simultaneous staining for F-actin and vinculin (compare *c* with *e*). Unstimulated D1 cells shown subcortical actin aggregates, as visualized by phalloidin staining (Fig. 6 *e*). After TNFα treatment, D1 cells undergo a profound change in shape and lose both the large membrane expansions and adhesiveness (Fig. 6 *b*). Vinculin is disassembled (Fig. 6 *d*) and polymerized F-actin is no longer detectable (Fig. 6 *f*). However, equal levels of vinculin protein were detected in both TNFα treated and untreated D1 cells, as shown by western blot analysis (Fig. 6 *d*, *inset*). In contrast to the disassembly of the actin filaments organization, microtubules are only partially affected by TNFα treatment (Fig. 6, *g* and *h*). The centriolar organization of microtubules appear to be more prominent after TNFα treatment.

The Ability of DC to Become Highly Mobile Correlates with their Functional Maturation. Migratory properties are essential to DC function and can be followed in vitro by time-lapse videomicroscopy. D1 cells, continuously observed for 2 h were moderately motile, but after treatment with TNFα they acquired a veiled morphology and became highly mobile within 1–2 h. On the average TNFα-treated, mature D1 cells migrated ~30–40 μ within 10 min (data not shown) with a broad range of individual mean velocities (2–5 μ/min). The migration paths were characterized by directional motility with changes in directions as if there was an ongoing scanning process of the surrounding microenvironment.

Very few cell divisions were observed during the 14-h experimental period, whereas frequent cell divisions were seen in the untreated D1 cells. This functional maturation process is likely to be irreversible at the single-cell level, but as the D1 population is heterogeneous (containing progenitors, immature and mature DC) self-regeneration occurs continuously.

Immature DC Acquire Antigens through Fluid Phase and Receptor-mediated Endocytosis with Higher Efficiency as Compared to Mature DC. Unstimulated D1 cultures were very efficient in fluid phase and receptor-mediated antigen uptake, a property largely abolished when the experiments were performed at 0°C. Using double-color FACS® analysis, the uptake at 37°C of FITC-OVA and FITC-DX was analyzed in the MHC class II^{int} and in the MHC class II^{bright} D1 cell subpopulations. The highest uptake of FITC-OVA and FITC-DX was associated with MHC class II ^{int} cells (Fig. 7). In contrast, the MHC class II ^{bright} D1 subpopulation was less efficient in FITC-OVA and FITC-DX uptake, thus indicating that macropinocytosis and receptor-mediated endocytosis are highly reduced in mature DC.

I-A^{bright} DC Are Superior to I-A^{int} Cells as Stimulators in the Primary MLR but Less Efficient in the Presentation of Native Exogenous Protein Antigen. 1 d after sorting, I-A^{bright} and I-A^{int} cells were used as stimulators of unprimed BALB/c lymphnode T lymphocytes. I-A^{bright} cells resulted much more potent activators of allogeneic T cells as compared to I-A^{int} cells (Fig. 8 *a*), in agreement with the notion that mature DC acquire a stronger stimulatory activity. However the situation may be different for nominal class II–restricted protein antigens. Immature murine DC were in fact reported to present native protein antigens better than short-term cultured DC (19). To address this issue, I-A^{bright} and I-A^{int} sorted cells were compared for their capacity to process and present native OVA or OVA peptides to the specific T hybridoma BO97.10. Sorted I-A^{int} cells were more efficient in the presentation of native OVA whereas both I-A^{bright} and I-A^{int} cells were very efficient in the presentation of the peptide to the same hybridoma (data not shown).

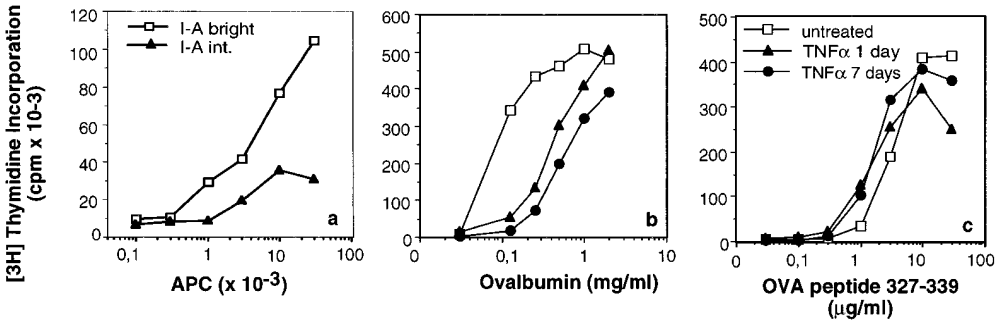

Figure 8. Allostimulatory and processing capacities of D1 cells. (*a*) Mixed lymphocyte reaction (MLR) by sorted I-A^{bright} and I-A^{int} D1 cells shows that the mature I-A^{bright} cells are the ones that have the highest allostimulatory capacity. Presentation of the OVA protein is downregulated by TNFα treatment. Antigen-specific presentation of exogenous OVA protein (*b*) or OVA-$peptide_{327-339}$ (*c*) by D1 cells treated or not with TNFα for 1 or 7 d: presentation of the OVA peptide is not affected by maturation but presentation of the OVA protein is downregulated by TNFα.

To test whether TNFα regulates antigen presentation, D1 cells were employed either untreated or after pretreatment with TNFα for 24 h, or for 7 d. The presentation of OVA protein was reduced (about one log) by pretreatment with TNFα, especially in the presence of lower antigen concentrations (Fig. 8 *b*). This result is likely to reflect the different processing abilities of immature versus mature DC populations. In contrast, both populations were able to present, with similar efficiencies, the OVA peptide (Fig. 8 *c*).

The Ability of DC to Produce IL-12 p75 Correlates with its Functional Maturation. Bioactive IL-12 p75 is the regulatory cytokine which drives the development of Th1 cells and promotes cell-mediated immunity. IL-12 p75 production by TNFα-treated or untreated D1 cells was measured in a presentation assay in the presence of OVA-specific T cell hybridoma (BO97.9). Immature D1 cells fail to produce IL-12 p75 constitutively or upon stimulation with heat-treated *S. aureus* and IFNγ (data not shown) or in the presence of the BO97.10 hybridoma (Fig. 9). In contrast, IL-12 p75 secretion was readily detectable in TNFα-matured D1 cells after interaction with antigen-specific T cell hybridoma. This result indicates that the feedback between T cells and DC is mediated by TCR-peptide/class II interaction. In order to exert this property, DC need to reach a stage of functional maturation which is not met by immature DC.

Discussion

DC originating from bone marrow cells, which include CFU-DC that yield homogeneous DC colonies under particular cytokine conditions (23), enter the blood as progenitors and colonize, from the blood stream, lymphoid, and non-lymphoid tissues. Spleen DC were identified for the first time by Steinman in 1979 (24) and were shown to be the predominant stimulators in the MLR reaction (25). In spite of two decades of studies, the DC differentiation process remains an unsolved issue and many key questions are still under investigation. Are DC progenitors predetermined to differentiate into fully mature DC and is this commitment irreversible? What are the functions that correlate with the various DC differentiation stages? To address some of these questions, the differentiation potential of immature spleen DC was investigated with the purpose to reproduce in vitro the process of DC differentiation and define the checkpoints of the so-called DC maturation.

We established an homogeneous immature DC population driven to proliferate for as long as growth factors are provided. These long-term, growth factor–dependent immature DC cells could be induced to mature in vitro, upon activation with a number of regulatory signals, into terminally differentiated DC. Using this defined model system, we identified three sequential stages of the DC maturation: stage 1 is adherent and characterized by a high proliferation rate, a low motility, and a highly organized cytoskeleton. The expression of MHC class II molecules seems to be mainly restricted to cytoplasmic vesicles positive for H2-Mβ

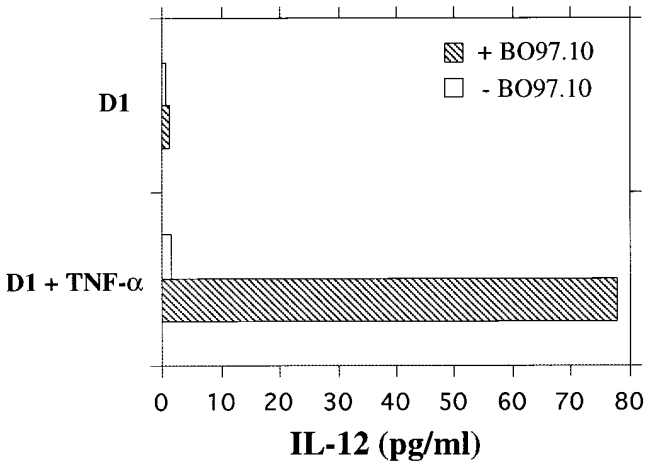

Figure 9. IL-12 p75 production by D1 cells pretreated or not with TNFα upon presentation of OVA protein to the specific hybridoma BO97.10 (*striped bars* or in the absence of the hybridoma *open bars*). IL-12 p75 was measured using an ELISA as described in Material and Methods. Il-12 p75 was quantified from two to three titration points using standard curves generated by purified recombinant mouse IL-12 and results expressed as cytokine concentration in pg/ml. Detection limit was 10 pg/ml.

molecules thus indicating that the majority of the class II molecules are located in a compartment similar to the MHC. CD40 and B7.2 costimulatory molecules are expressed at low level. Furthermore, these immature DC are inefficient in allostimulatory activity and are unable to secrete IL-12 but have a high capacity of antigen uptake and processing.

Progression from stage 1 towards stage 2 requires signaling, and this can be achieved using living bacteria, LPS or cytokines such as TNFα or IL-1β but not IL-6. Stage 2, which is induced in few hours and is completed after one day, is characterized by low proliferative rate, high motility, and complete depolarization of actin cytoskeleton with loss of adhesiveness. In addition, mature DC rearrange the cell surface expression of receptors and molecules: MHC class II, CD-40, and B7.2 molecules become highly expressed on the cell surface and this may correlate with the ability to produce IL-12.

Interestingly, intracellular class II–containing compartments appear to be different from the ones observed in immature D1 cells, given that colocalization with the H2-Mβ molecule is no longer detectable. In contrast, mature DC disassemble actin-based cytoskeleton, lose adhesion plaques, and become inefficient in protein antigen uptake and presentation. However, allostimulatory activity and peptide presentation remain very efficient.

Most of these cells will spontaneously progress towards stage 3 where they completely stop proliferation. In agreement with this hypothesis we also found that MHC class II^{high} sorted D1 cells, if recultured after sorting, enter stage 3, characterized by cell growth arrest and final cell death by apoptosis. In contrast, sorting and reculture of the MHC class II^{int} D1 subpopulation leads to the development of a population which resembles the initial bulk D1 cells. Thus, the D1 bulk population contains self-renewal progenitors from which both immature and mature DC can be easily generated.

All the stages of this sequential maturation are relevant for experimental therapeutics and transplantation biology. In fact, the growth of heterogeneous bulk DC populations or selected immature DC, may be more suitable for experimental therapeutics than the growth of selected fully mature DC undergoing terminal differentiation. We have shown that native proteins are better presented by immature DC whereas peptides are better presented by mature DC. Therefore, design of therapeutical approaches based either on protein or peptide DC loading should carefully consider the stage of DC maturation; to select the most suitable DC subpopulation the purification procedures should be well defined as well as the culture conditions in order to preserve either immature or mature DC. Which factors preserve the self-renewal potential of the progenitors and what prevents the full maturation of the D1 cells (in the culture conditions described above) are still open questions, presently under investigation.

Our data concerning the process of DC maturation are in agreement with a number of studies (2, 3, 5, 9, 10, 13, 23, 26) but are in contrast with some others. In particular, the current view of a full interconversion between mature DC and macrophages (27) should be carefully examined at the single cell level using homogeneous cell populations, such as the D1 cells. The DC phenotype could not be reversed into a macrophage one, indicating that once the bulk DC population is committed to the DC phenotype this process is irreversible. When the purification procedures can not separate shared precursors (likely to be in common with monocytes) the lineage commitment is more difficult to be observed.

What stimuli induce full differentiation of mouse DC? In this study we provide the first evidence that TNFα plays a crucial role in mouse DC maturation, as previously reported in human monocyte-derived (13) and bone marrow–derived DC (23), as well as in LC (7). We also showed that IL-1β induces phenotypical DC maturation, most likely through a paracrine induction of TNFα expression, as shown in LC (6, 28, 29). Living bacteria and bacterial cell constituents are also strong inducers of full DC maturation, including upregulation of the costimulatory molecules B7.2 and CD40. It is likely that in vivo, the first signals inducing DC maturation are delivered by microbes since we previously showed a paracrine induction of TNFα expression in DC infected with $Gram^+$ and $Gram^-$ bacteria (30). Thus, TNFα is most likely a signal 2 for sequential DC maturation, whereas pathogens represent a signal 1.

In addition to its function in DC morphological maturation, TNFα also promotes DC emigration (4) from tissues such as skin, intestine, heart, and kidney (4, 29, 31, 32). The non-lymphoid DC need to move on to the regional lymph nodes in order to encounter naive T cells and elicit primary immune responses. Thus, the migratory properties are an essential component of the DC function. In this report we also provide the first evidence that TNFα is able to induce a complete rearrangement of the actin-based cytoskeleton in DC.

This actin disassembly could explain the decreased macropinocytosis ability of mature DC as proposed in other systems (33). The disassembly of actin filaments upon TNFα treatment is correlated with a loss of endocytic capacity in DC. Macropinocytosis represents one of the most efficient antigen uptake mechanism in DC but requires the integrity of polymerized actin filaments; it is likely that DC maturation shuts off the micropynocytic pathway by inducing actin disassembly. The modification of the actin cytoskeleton is also relevant in the acquisition of migration properties of mature DC. TNFα treatment induces cell detachment and formation of an organized centriolar array of microtubules which are likely to be highly dynamic (34). Membrane expansions of mature DC, which occur in response to the cytoskeleton remodeling, also appear highly dynamic: vinculin containing adhesive structures disappear and the cells acquire migratory properties. By time-lapse videomicroscopy we were able to show the highly enhanced motility of the TNFα-activated D1 cells. Because F-actin seems to be mainly disorganized, whereas microtubules are still highly organized, our data indicate a role for microtubules in determining DC movements. In vivo, motility should unable

DC to encounter T cells and the final outcome should be T cell activation and Th1/Th2 polarization. It has been proposed that DC maturation continues until DC-T cell interaction occurs (35) but in the D1 model mature DC were driven to terminal differentiation even in the absence of T cells. On the other hand, interaction of DC with T cells was essential for IL-12 production (this study and 36). Interestingly, immature DC fail to produce IL-12 p75 either upon stimulation with heat treated *S. aureus* and IFNγ or after activation with antigen-specific T cell hybridoma. In contrast, IL-12 p75 secretion is readily detectable in TNFα-treated DC after interaction with antigen-specific T cells. This result indicates that the feedback between T cells and DC is dependent on TCR-peptide/class II interaction and this property is reached at stage 2 of functional maturation. These data also indicate that DC may play a major role in polarizing the immune response towards the Th1 pathway.

The model system analyzed in this study reproduces DC differentiation in vitro from the very early events towards terminal maturation. A fine molecular analysis of each step of functional DC maturation can now be undertaken.

We wish to thank Giampiero Girolomoni for critical readings, Domenico Delia for cell sorting, and Carmela Mutini, Fabrizio Manca and Daniele Severino for time-lapse videomicroscopy. Peptide 327-339 was kindly synthesized by Renato Longhi; Donata Medaglini and Gianni Pozzi kindly provided the bacteria used in this study. A special thanks to Elena Bottani for careful editing of the manuscript.

This work was supported by the Italian Ministry of Public Health (Istituto Superiore di Sanità: AIDS grant 9403-92 and MS grant 52), by the National Council Research (CNR), by Biotop, and by the French Association against Cancer, grant 6058 (ARC).

Address correspondence to Paola Ricciardi-Castagnoli, CNR (National Council Research) Centre of Cellular and Molecular Pharmacology, Via Vanvitelli 32, 20129 Milano, Italy.

Received for publication 24 September 1996 and in revised form 12 November 1996.

References

1. Steinman, R.M. 1991. The dendritic cell system and its role in immunogenicity. *Annu. Rev. Immunol.* 9:271–296.
2. Schuler, G., and R.M. Steinman. 1985. Murine epidermal Langerhans cells mature into potent immunostimulatory dendritic cells in vitro. *J. Exp. Med.* 161:526–546.
3. Inaba, K., M. Witmer-Pack, M. Inaba, K.S. Hathcock, H. Sakuta, M. Azuma, H. Yagita, K. Okumura, P.S. Linsley, S. Ikehara et al. 1994. The tissue distribution of the B7-2 costimulator in mice: abundant expression on dendritic cells in situ and during maturation in vitro. *J. Exp. Med.* 180:1849–1860.
4. Roake, J.A., A.S. Rao, P.J. Morris, C.P. Larsen, D.F. Hankins, and J.M. Austyn. 1995. Dendritic cell loss from nonlymphoid tissues after systemic administration of lipopolysaccharide, tumor necrosis factor, and interleukin 1. *J. Exp. Med.* 181:2237–2247.
5. Witmer-Pack, M.D., W. Olivier, J. Valinsky, G. Schuler, and R.M. Steinman. 1987. Granulocyte/macrophage colony-stimulating factor is essential for the viability and function of cultured murine epidermal Langerhans cells. *J. Exp. Med.* 166:1484–1498.
6. Heufler, C., F. Koch, and G. Schuler. 1988. Granulocyte/macrophage colony-stimulating factor and interleukin 1 mediate the maturation of epidermal Langerhans cells into potent immunostimulatory dendritic cells. *J. Exp. Med.* 167: 700–712.
7. Caux, C., D. Dezutter-Dambuyant, D. Schmitt, and J. Banchereau. 1992. GM-CSF and TNF-α cooperate in the generation of dendritic Langerhans cells. *Nature (Lond.).* 360: 258–261.
8. Scheicher, C., M. Mehlig, R. Zecher, and K. Reske. 1992. Dendritic cells from mouse bone marrow: in vitro differentiation using low doses of recombinant granulocyte/macrophage CSF. *J. Immunol. Methods* 154:253–264.
9. Inaba, K., M. Inaba, N. Romani, H. Aya, M. Deguchi, S. Ikehara, S. Maramatsu, and R.M. Steinman. 1992. Generation of large numbers of dendritic cells from mouse bone marrow cultures supplemented with granulocyte/macrophage colony-stimulating factor. *J. Exp. Med.* 176:1693–1702.
10. Inaba, K., R.M. Steinman, M. Witmer-Pack, H. Aya, M. Inaba, T. Sudo, S. Wolpe, and G. Schuler. 1992. Identification of proliferating dendritic cells in mouse blood. *J. Exp. Med.* 175:1157–1167.
11. Romani, N., S. Gruner, D. Brang, E. Kämpgen, A. Lenz, B. Trockenbacher, G. Konwalinka, P.O. Fritsch, R.M. Steinman, and G. Schuler. 1994. Proliferating dendritic cell progenitors in human blood *J. Exp. Med.* 180:83–93.
12. Szabolcs, P., M.A. Moore, and J.W. Young. 1995. Expansion of immunostimulatory dendritic cells among the myeloid progeny of human $CD34^+$ bone marrow precursors cultured with c-kit ligand, granulocyte-macrophage colony-stimulating factor, and TNF-α. *J. Immunol.* 154:5851–5861.
13. Sallusto, F., and A. Lanzavecchia. 1994. Efficient presentation of soluble antigen by cultured human dendritic cells is maintained by granulocyte/macrophage colony stimulating factor plus interleukin 4 and downregulated by tumor necrosis factor-α. *J. Exp. Med.* 179:1109–1118.
14. Elbe, A., S. Schleischitz, D. Strunk, and G. Stingl. 1994. Fetal skin-derived MHC class I^+, MHC class II^- dendritic cells stimulate MHC class I-restricted responses of unprimed $CD8^+$ T cells. *J. Immunol.* 153:2878–2889.
15. Xu, S., K. Ariizumi, G. Caceres-Dittmar, D. Edelbaum, K. Hashimoto, P.R. Bergstresser, and A. Takashima. 1995. Successive generation of antigen-presenting, dendritic cell lines

from murine epidermis. *J. Immunol.* 154:2697–2705.
16. Guéry, J.C., F. Ria, and L. Adorini. 1996. Dendritic cells but not B cells present antigenic complexes to class II–restricted T cells after administration of protein in Gavrieli, Y., Y. Sherman, and S.A. Ben-Sasson. 1992. identification of programmed cell death in situ via specific labeling of nuclear DNA fragmentation. *J. Cell Biol.* 119:493–501.
17. Humbert, M., G. Raposo, P. Cosson, H. Reggion, J. Davoust, and J. Salamero. 1993. The invariant chain induces compact forms of class II molecules localised in late endosomal compartments. *Eur. J. Immunol.* 23:3158–3166.
18. Dutartre, H., J. Davoust, J.P. Gorvel, and P. Chavrier. 1996. Cytokinesis arrest and redistribution of actin-cytoskeleton in cells expressing the Rho GTPase CDC42Hs. *J. Cell Sci.* 109: 367–377.
19. Lutz, M.B., C.U. Aßmann, G. Girolomoni, and P. Ricciardi-Castagnoli. 1996. Different cytokines regulate antigen uptake and presentation of a precursor dendritic cell line. *Eur. J. Immunol.* 26:586–594.
20. Ishioka, G.Y., L. Adorini, J.C. Guery, F.C.A. Gaeta, R. LaFond, J. Alexander, M.F. Powell, A. Sette, and H.M. Grey. 1994. Failure to demonstrate long-lived MHC saturation both in vitro and in vivo. *J. Immunol.* 152:4310–4316.
21. Gately, M.K., R. Chizzonite, and D.H. Presky. 1995. Measurement of human and mouse IL-12. *Curr. Prot. Immunol.* 3: 15:6 and 3:16:1.
22. Takashima, A., D. Edelbaum, T. Kitajima, R.K. Shadduck, G.L. Gilmore, S. Xu, R.S. Taylor, P.R. Bergstresser, and K. Ariizumi. 1995. Colony-stimulating factor-1 secreted by fibroblasts promotes the growth of dendritic cell lines (XS series) derived from murine epidermis. *J. Immunol.* 154:5128–5135.
23. Young, J., W. Szabolcs, and M.A.S. Moore. 1995. Identification of dendritic cell colony-forming units among normal human $CD34^+$ bone marrow progenitors that are expanded by c-kit-ligand and yield pure dendtritic cell colonies in the presence of granulocyte/macrophage colony-stimulating Factor and Tumor Necrosis Factor α. *J. Exp. Med.* 182:1111–1120.
24. Steinman, R.M., G. Kaplan, M.D. Witmer, and Z.A. Cohn. 1979. Identification of a novel cell type in peripheral lymphoid organs of mice V. Purification of spleen dendritic cells, new surface markers, and maintenance in vitro. *J. Exp. Med.* 149:1–16.
25. Ahmann, G.B., P.I. Nadler, A. Birnkrant, and R.J. Hodes. 1979. Non-T radiation resistant splenic adherent cells are the predominant stimulators in the murine mixed lymphocyte reaction. *J. Immunol.* 123:1903–1909.
26. Sallusto, F., and A. Lanzavecchia. 1995. dendritic cells use macropinocytosis and the mannose receptor to concentrate macromolecules in the major histocompatibility complex class II compartment: downregulation by cytokines and bacterial products. *J. Exp. Med.* 182:389–400.
27. Peters, J.H., R. Gieseler, B. Thiele, and F. Steinbach. 1996. Dendritic cells: from ontogenetic orphans to myelomonocytic descendants. *Immunol. Today.* 17:273–278.
28. Koide, S.L., K. Inaba, and R.M Steinman. 1987. IL-1 enhances T-dependent immune responses by amplifying the function of dendritic cells. *J. Exp. Med.* 165:515–530.
29. Cumberbatch, M., and I. Kimber. 1995. TNFα is required for accumulation of dendritic cells in draining lymph nodes and for optimal contact sensitization. *Immunology.* 84:31–35.
30. Riva, S., M.L. Nolli, M.B. Lutz, S. Citterio, G. Girolomoni, C. Winzler, and P. Ricciardi-Castagnoli. 1996. Bacteria and bacterial cell wall constituents induce the production of regulatory cytokines in dendritic cell clones. *J. Inflamm.* 46:98–105.
31. Larsen, C.P., P.J. Morris, and J.M. Austyn. 1990. Migration of dendritic leukocytes from cardiac allografts into host spleens, a novel pathway for initiation of rejection. *J. Exp. Med.* 171:307–314.
32. Larsen, C.P., and J.M. Austyn. 1990. Migration and Maturation of Lagerhans cells in skin. *Transplants and Explants.* 172: 1483–1493.
33. Pfeiffer, J.R. J.C. Scagrve, B.H. Davis, G.G. Deanim, and J.M. Oliver. 1985. Membrane and cytoskeleton changes associated with IgE-mediated serotonin release from rat basophlic leukemia. *J. Cell. Biol.* 101:2145–2155.
34. Pepperkok, R., M.H. Bre, J. Davoust, and T.E. Kreis. 1990. Microtubules are stabilized in confluent ephitelial cells but not in fibroblasts. *J. Cell. Biol.* 111:3003–3012.
35. Caux, C., C. Massacrier, B. Vanbervliet, B. Dubois, C. Van Kooten, I. Durand, and J. Banchereau. 1994. Activation of human dendritic cells through CD40 cross-linking. *J. Exp. Med.* 180:1263–1272.
36. Heufler, C. , F. Koch, U. Stanzl, G. Topar, M. Wysocka, G. Trinchieri, A. Enk, R.M. Steinman, N. Romani, and G. Schuler. 1996. Interleukin-12 is produced by dendritic cells and mediates T helper 1 development as well as interferon-γ production by T helper 1 cells. *Eur. J. Immunol.* 26:659–668.
37. Paddock, S.W. 1989. Tandem scanning reflected-light microscopy of cell-substratum adhesions and stress fibers in Swiss 3T3 cells. *J. Cell Sci.* 93:143–146.